ARTICLE

Two-Dimensional Molecular Crystals of Phosphonic Acids on Graphene

Mariana C. Prado, Regiane Nascimento, Luciano G. Moura, Matheus J. S. Matos, Mario S. C. Mazzoni, Luiz G. Cancado, Helio Chacham, and Bernardo R. A. Neves*

Departamento de Física, ICEx, Universidade Federal de Minas Gerais-UFMG, C.P. 702, 30123-970, Belo Horizonte, Brazil

ABSTRACT The synthesis and characterization of two-dimensional (2D) molecular crystals composed of long and linear phosphonic acids atop graphene is reported. Using scanning probe microscopy in combination with first-principles calculations, we show that these true 2D crystals are oriented along the graphene armchair direction only, thereby enabling an easy determination of graphene flake orientation. We have also compared the doping level of graphene flakes *via* Raman spectroscopy. The presence of the molecular crystal atop graphene induces a well-defined shift in the Fermi level, corresponding to hole doping, which is in agreement with our *ab initio* calculations.

KEYWORDS: graphene · phosphonic acids · electronic structure · self-assembly · surface modification

From graphene, nothing less than a revolution in the electronics industry is expected.[1] To achieve such a breakthrough, many basic issues need to be first addressed, such as the control of its energy band gap and its doping levels. Band-gap engineering has been proposed through nanoribbon fabrication, use of bilayers, or even strain application.[2−4] Variation of graphene doping levels is easy to accomplish, as it is very sensitive to environmental conditions, but full control of the doping level is more elusive. Here, we show the synthesis and characterization of two-dimensional (2D) molecular crystals of phosphonic acids atop graphene. These true 2D crystals are oriented along the graphene armchair direction only. The doping level of graphene flakes, before and after the molecular crystal deposition, was monitored *via* Raman spectroscopy. The graphene decoration with octadecylphosphonic acid (OPA) molecular crystals produces an unambiguous hole-doping, with carrier concentrations of $\rho \sim 10^{13}$ cm^{-2}.

To manipulate graphene's electronic properties, several routes, such as its chemical modification (like in the synthesis of graphane)[5] or its functionalization (such as decoration with organic molecules),[6−8] have been proposed. This latest route relies on the capability of many organic molecules to form self-assembled monolayers (SAMs) because one of the key appeals of SAMs is their ability to modify the surface properties of the supporting substrate.[6−10] Because the final properties of the substrate−SAM system depend primarily on molecule−substrate, molecule−molecule, and molecule−environment interactions, a myriad of organic molecules—with different sizes, geometries, head- and tail groups—has been proposed for tailoring the desired surface properties.[9,10] Silanes on silicon oxide and thiols on gold surfaces are the most studied SAM systems,[9,10] but phosphonic acids are also known to form well-defined self-assembled structures on a variety of substrates.[11−14] Because graphene is a prototypical surface-only (or 2D) material, the idea of associating well-chosen SAMs to manipulate some of its properties seems to be natural. Nevertheless, so far, only a few studies[6−8] have explored the idea of graphene modification through SAM-forming molecules. References 7 and 8 report the electrical characterization of SAM−graphene systems, identifying molecular-induced doping but showing no evidence of molecular organization. Reference 6 reports the crystalline organization of molecules atop graphene, but without any register between the orientation of the molecular crystal domains and the orientation of graphene. Within such a framework, this work brings experimental and theoretical results that demonstrate the realization of well-organized monolayers (or 2D crystals), formed by linear phosphonic acid molecules, on

*Address correspondence to bernardo@fisica.ufmg.br.

Received for review August 30, 2010 and accepted December 14, 2010.

Published online December 27, 2010. 10.1021/nn102211n

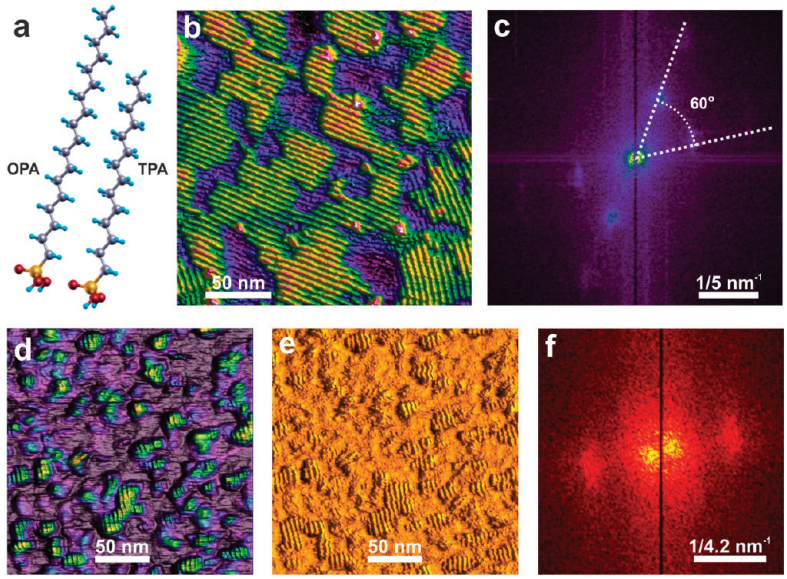

Figure 1. AFM characterization of 2D phosphonic acid crystals atop graphene single and multilayers. (a) Schematic representation of both phosphonic acids employed in this work: the octadecylphosphonic acid (OPA), which is 2.5 nm long, and the tetradecylphosphonic acid (TPA), which is 2.1 nm long. (b) AFM-topography image of 2D OPA crystals (green-yellow) partially covering a multilayer graphene (blue-purple). (c) Fast Fourier transform of the previous image, showing well-defined periodicity and angle between OPA crystals. (d) AFM-topography and (e) AFM-phase images of 2D TPA crystals partially covering a graphene monolayer. (f) Fast Fourier transform of the image in (e) evidencing the regular periodicity of the TPA crystals. Some periodic features are also seen in certain purple regions of image (b). These are simply color rendering artifacts, caused by the natural corrugation of the sample. Therefore, such periodic (purple) regions are, indeed, also OPA-covered regions and not the bare graphene, which shows no periodicity.

graphene. Being oriented along the graphene armchair direction only, these crystals enable an easy determination of graphene flake orientation. Moreover, the presence of the molecular crystal atop graphene induces a well-defined p-type doping. Our results indicate that an appropriate choice of molecule parameters, such as geometry, length, and headgroup chemistry, may represent a viable option for an efficient tuning of graphene electronic properties.

RESULTS AND DISCUSSION

Figure 1 summarizes the morphological atomic force microscopy (AFM) characterization of the phosphonic acid 2D crystals deposited on graphene (mono- and multilayers). Figure 1a shows schematic drawings of both molecules investigated in this work: octadecylphosphonic acid (OPA) and tetradecylphosphonic acid (TPA), which have a phosphonic acid headgroup attached to a long and linear alkyl chain terminated by a methyl group.[11,13] In previous studies, we have shown that these molecules form well-organized self-assembled monolayers and bilayers on a variety of substrates.[12−14] More specifically, Fontes[14] shows that both TPA and OPA form well-ordered structures atop nonpolar surfaces, such as HOPG, whereas shorter molecules form amorphous agglomerates on the same substrates. Therefore, we prepared a series of graphene samples (mono- to multilayers) that were spread-coated with OPA or TPA solutions. In the topographic AFM image of Figure 1b, the multilayered graphene substrate (in purple) is partially covered with a single layer of well-defined OPA rippled domains (in green-yellow). The thickness of a rippled domain is around 0.3−0.5 nm. The ripples in Figure 1b are periodically spaced and exist at fixed directions only. Indeed, the fast Fourier transform (FFT) of this image, shown in Figure 1c, clearly indicates a 5 nm periodicity (twice the OPA length, in agreement with X-ray data for OPA self-assembled bilayers)[13,14] and that different orientation domains, as those in the bottom right and left of Figure 1b, form a precise angle of 60° with the orientation of the others.

Figure 1d,e shows AFM (topography and phase, respectively) images of a monolayer graphene flake partially covered with TPA ripple domains. The FFT image in Figure 1f shows that these domains are aligned in one direction only and that their ripple periodicity is 4.2 nm (twice the length of the TPA molecule). Even though some ripple domains are not clearly seen in the topography image (Figure 1d), they are clearly visible in the phase image (Figure 1e). This fact is a consequence of the natural roughness of a monolayer of graphene atop the SiO_x surface, which, in our samples, is of the order of 0.3 nm, thus causing a blurring effect on the topographic image. The phase image is less sensitive to topographic variations at this scale and more sensitive to energy dissipation mechanisms (which are material-dependent).[15] Therefore, a good contrast is always achieved in the phase images, even when the topographic image is faint.

In a previous study, Fontes suggested that the OPA and TPA rippled domains observed on the HOPG sur-

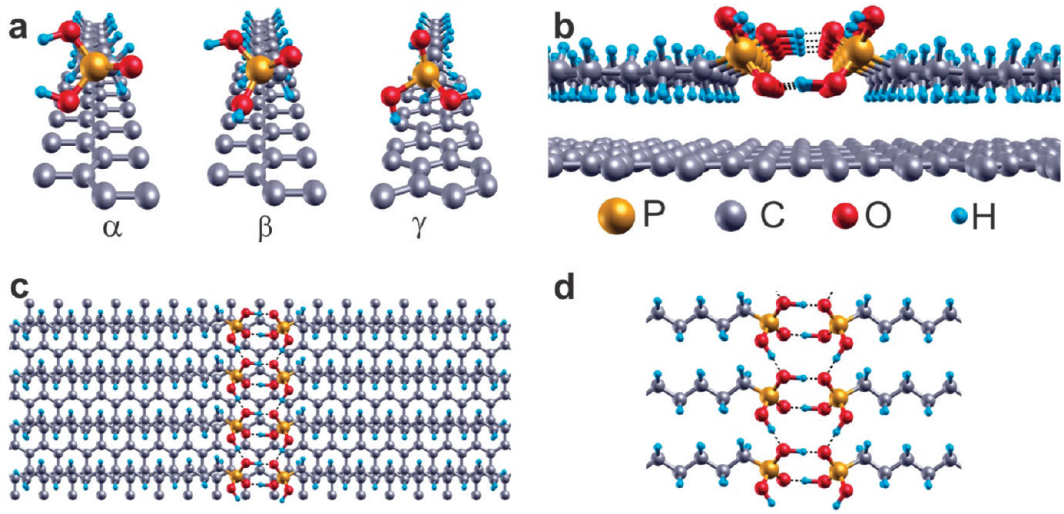

Figure 2. Calculated TPA structures atop graphene. (a) Three examples of unit cells of optimized TPA/graphene structures. α and β are structures with the TPA alkyl chain oriented along the graphene zigzag direction, and γ is an armchair-oriented structure. (b−d) Detailed views of the most stable structure obtained in our calculations, in a repeated (4 × 1) unit cell. In (d) (a zoom-in of (c)), the underlying graphene layer was removed in order to make the geometry of the TPA headgroup hydrogen bonding clearer.

face are horizontal bilayers, in analogy with conventional vertical bilayers.[14] Therefore, to confirm the nature of the OPA and TPA rippled domains seen in Figure 1, we performed first-principles calculations of the structural properties of single layers of TPA and OPA dimers atop graphene. We considered crystalline assemblies with two possible molecule orientations: along either the zigzag or the armchair graphene directions. In each case, we chose the two-dimensional crystal unit cell that best matches the observed lattice parameters for OPA and TPA/graphene systems. In Figure 2a, we show two zigzag-oriented structures and an armchair-oriented one. We considered several initial molecular configurations for the TPA/graphene system and optimized those geometries. This resulted in eight distinct TPA/graphene structures, four along each direction. The relaxation resulted in three distinct configurations of the $PO(OH)_2$ headgroup of the TPA and OPA molecules. These are shown in Figure 2a and labeled as α, β, and γ.

We compared the energetic stability of the TPA/graphene and OPA/graphene structures through their formation energies. The results (see the Supporting Information) indicate that the most stable configuration (for both TPA and OPA) is the one with the alkyl chain along the zigzag direction, with the $PO(OH)_2$ in the β configuration, and with the TPA (or OPA) carbon atoms parallel to graphene, as shown in Figure 2b−d for the TPA case. Figure 2c shows that the position of TPA atop graphene is such that half of the hydrogen atoms of the TPA alkyl chain approximately fit atop the center of graphene hexagons. Such a structure, which was not imposed in the initial configuration, coincides with Groszek's model for hydrocarbons atop graphite.[16] In Figure 2b,d, one can see the relative orientation of neighboring $PO(OH)_2$ headgroups for the most stable β configuration. This orientation and the length of the translation vector are such that they allow the formation of hydrogen bonds among neighboring $PO(OH)_2$ headgroups, as evidenced in Figure 2b,d.

On comparison of Figures 1 and 2, it is clear that the observed ripples in Figure 1 are formed by the well-ordered phosphonic acid dimers in Figure 2c, with a perfect registry with the underlying graphene layer. Considering that the most stable OPA and TPA structures with the alkyl chain along graphene's zigzag direction have much lower formation energies than those along the armchair direction (see the Supporting Information) and that the ripple direction is perpendicular to that of the alkyl chains, we conclude that all ripples in Figure 1 are oriented along the armchair direction of graphene. That is, the graphene crystalline orientation is revealed by the 2D phosphonic acid crystal orientation, without the need of tedious ultra-high-vacuum, high-resolution SPM experiments.

We have also investigated the occurrence of charge transfer between graphene layers and the 2D molecular crystals *via ab initio* calculations and Raman scattering experiments. Our theoretical results show that, in all cases, electrons are transferred from graphene to the phosphonic acid, resulting in p-doped graphene. In the case of TPA, the most stable structure (see the Supporting Information) leads to a charge density of 5.0×10^{13} cm^{-2} and, in the case of OPA, 5.3×10^{13} cm^{-2}. Considering all the 11 investigated structures for both OPA and TPA (also see the Supporting Information), the induced charge density ranges from 3.6×10^{13} to 5.3×10^{13} cm^{-2}. Figure 3 shows two Raman spectra obtained from the same region of a monolayer graphene flake (see the top-right inset in Figure 3 and the Supporting Information). The upper spectrum (black curve) and the bottom spectrum (red curve) were obtained before

and after the deposition of the OPA molecules, respectively. Both spectra show two major Raman features: the first-order bond-stretching G band[18] and two-phonon G′ band.[19] The single-Lorentzian shape of the G′ band (~2690 cm^{-1}) reassures that the graphene piece is a single-layer flake.[19]

The difference between the two spectra depicted in Figure 3 undoubtedly confirms the occurrence of a shift in the Fermi level caused by chemical doping. Before the OPA deposition, we have measured $\nu_G = 1586$ cm^{-1} and $W_G = 15$ cm^{-1} (ν_G and W_G stand for the G band frequency and full width at half-maximum, respectively). According to ref 20, where the authors have systematically monitored the G and G′ bands parameters by tuning the gate voltage in a top-gated graphene transistor, these values indicate that the graphene flake was slightly doped before the OPA deposition ($\rho \sim 0.2 \times 10^{13}$ cm^{-2}). After the OPA deposition, we have measured $\nu_G = 1593$ cm^{-1} and $W_G = 10$ cm^{-1}, which, compared to the values reported in ref 20, leads to $\rho \sim 1.2 \times 10^{13}$ cm^{-2}. Notice that the value obtained for the charge concentration, ρ, is consistent with the value predicted from our *ab initio* calculations ($\rho \sim 5.3 \times 10^{13}$ cm^{-2}).

Another strong evidence of chemical doping observed in the Raman spectra shown in Figure 3 is a reduction of about 60% of the ratio between the intensities (peak heights) of the G′ and G bands after the OPA deposition.[17,20,21] According to ref 21, this reduction is related to a decrease on the G′ band intensity due to an increase on the probability of the photogenerated electron−hole pairs to undergo inelastic scattering with doping-induced electron or holes. Notice that the disorder-induced D band (occurring at ~1350 cm^{-1} for experiments using a 514.5 nm laser line)[18] cannot be observed in both spectra shown in Figure 3, which means that (i) our graphene flake has a low defect density and (ii) the deposition process does not generate structural disorder in the graphene lattice.

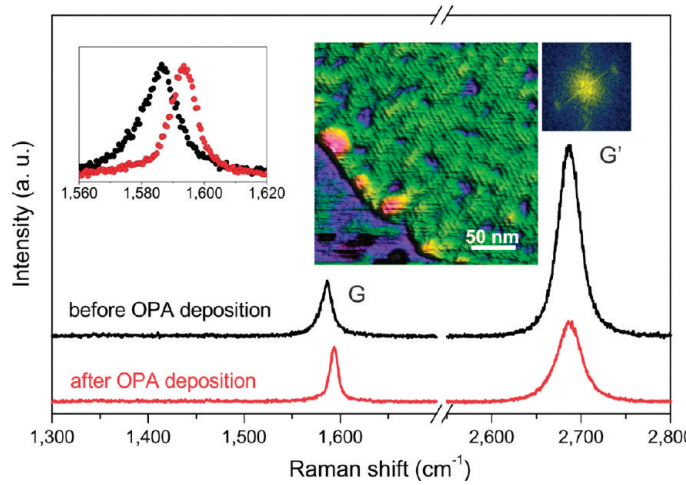

Figure 3. Raman spectroscopy data. Raman spectra obtained from the same region of a monolayer graphene flake (see the AFM image of the flake border and its respective FFT at the upper right of the figure) before (black curve) and after (red curve) deposition of OPA molecules. The inset at the top left shows the superposition of the G band obtained in both cases (dark circles for the spectrum obtained before OPA deposition and red circles for the spectrum obtained after OPA deposition) for better visualization. The stiffening and narrowing of the G band (clarified in the inset), combined with the drastic reduction of the ratio between the G and G′ band peak heights, undoubtedly confirms the presence of chemical doping after the OPA deposition.[17]

CONCLUSION

In summary, this work brings some important advances in the association of SAM-forming molecules and graphene: with the appropriate choice of molecule geometry (linear), length (long), and headgroup (highly polar), 2D crystals are spontaneously formed on the graphene surface. The natural corrugation of these crystals promptly reveals the graphene orientation under standard imaging conditions. They also induce a well-defined p-doping of graphene, without introducing any defects on its structure. The nanometric scale of the 2D crystal periodicity (4−5 nm) and its accompanying periodic potential may have important effects on the transport properties of graphene devices, as recently proposed in a theoretical work.[22] As shown by Fontes in an earlier work,[14] these 2D crystals should be, thermally, very stable on graphene, withstanding temperatures above 100 °C, as they do on graphite. A similar stability study, carried out with decorated epitaxial graphene, shows a persistent doping effect up to 200 °C.[7] The phosphonic acid structures are also robust upon illumination, as no sample modifications are observed before and after successive laser irradiation cycles during the Raman investigation. Therefore, with the vast amount of possibilities readily available, we believe that 2D crystals on graphene may open up a whole subfield of graphene research and application, enabling the correct tailoring of device characteristics, such as doping, crystallographic orientation, and fine-tuning of its optical and transport properties.

MATERIALS AND METHODS

Mono- to multilayer graphene samples were prepared by the mechanical exfoliation of graphite onto a 300 nm thick Si oxide layer covering a p-doped Si substrate. These graphene flakes were initially identified using optical microscopy and, then, investigated by scanning probe microscopy using a Nanoscope IV MultiMode SPM, from Veeco Instruments operating in intermittent contact (tapping) mode. For some SPM and Raman tests, HOPG substrates were also employed. SPM measurements were carried out in air employing standard silicon cantilevers (Advanced-TEC, from Nanosensors; AC-160, from Olympus; NSG-11, from NT-MDT; and Tetra15, from K-Tek).

Octadecylphosphonic acid (OPA), $CH_3(CH_2)_{17}PO(OH)_2$, and tetradecylphosphonic acid (TPA), $CH_3(CH_2)_{13}PO(OH)_2$ (see Figure

1a), were used as purchased from Alpha Aesar to prepare ethanolic solutions with concentrations of 0.2 mM (TPA and OPA) and 0.4 mM (OPA).[12] The 2D crystals were prepared simply by drip-coating (or spread-coating) the SiO_x−graphene substrate with the appropriate phosphonic acid solution for 40 s, followed by drying with clean N_2.[12−14] It should be noted that no significant variations were observed in the self-assembled structures formed by the OPA solutions, for the different solution concentrations employed in this work.

Raman spectroscopy measurements were performed using a HORIBA Jobin Yvon T64000 triple-monochromator in the backscattering configuration. The laser spot size was 1 μm using a 100× objective, and the laser power was kept at 1.0 mW in order to avoid sample heating. Raman spectra were obtained using the 514.5 nm Ar laser line.

The *ab initio* calculations were based on the density functional theory[23] within the local density (LDA) approximation for the exchange-correlation functional, as implemented in the SIESTA method.[24] We make use of norm-conserving pseudopotentials in the Keinman−Bylander factorized form,[25] and a double-ζ basis set composed of finite-range numerical atomic pseudofunctions enhanced with polarization orbitals. A real-space grid is used with a mesh cutoff of 200 Ry. All geometries were optimized so that the maximum force on any atom is less than 0.025 eV.

Acknowledgment. The authors are grateful to Dr. Leonardo Campos for the sample preparation and to Prof. Marcos Pimenta for helpful discussions in the Raman data analysis. M.C.P., R.N., L.G.M., and M.J.S.M. are thankful to CNPq and CAPES for their scholarships. Financial support from Fapemig, CNPq, and INCT/Nanomateriais de Carbono is also acknowledged.

Supporting Information Available: The Supporting Information includes the details of the *ab initio* calculation, the results for the OPA/graphene structures, and the formation energies for the different TPA configurations. Also, AFM images of OPA atop graphene showing the monolayer coverage where the Raman spectra were acquired are also included. This material is available free of charge *via* the Internet at http://pubs.acs.org.

REFERENCES AND NOTES

1. Schwierz, F. Graphene Transistors. *Nat. Nanotechnol.* **2010**, *5*, 487.
2. Han, M.; Ozyilmaz, B.; Zhang, Y. B.; Kim, P. Energy Band-Gap Engineering of Graphene Nanoribbons. *Phys. Rev. Lett.* **2007**, *98*, 206805.
3. Ohta, T.; Bostwick, A.; Seyller, Th.; Horn, K.; Rotenberg, E. Controlling the Electronic Structure of Bilayer Graphene. *Science* **2006**, *313*, 951–954.
4. Pereira, V. M.; Castro Neto, A. H.; Peres, N. M. R. Tight-Binding Approach to Uniaxial Strain in Graphene. *Phys. Rev. B* **2009**, *80*, 045401.
5. Elias, D. C.; Nair, R. R.; Mohiuddin, T. M. G.; Morozov, S. V.; Blake, P.; Halsall, M. P.; Ferrari, A. C.; Boukhvalov, D. W.; Katsnelson, M. I.; Geim, A. K.; et al. Control of Graphene's Properties by Reversible Hydrogenation: Evidence for Graphane. *Science* **2009**, *323*, 610–613.
6. Wang, Q. H.; Hersam, M. C. Room-Temperature Molecular-Resolution Characterization of Self-Assembled Organic Monolayers on Epitaxial Graphene. *Nat. Chem.* **2009**, *1*, 206–211.
7. Coletti, C.; Riedl, C.; Lee, D. S.; Krauss, B.; Patthey, L.; Klitzing, K.; Smet, J. H.; Starke, U. Charge Neutrality and Band-Gap Tuning of Epitaxial Graphene on SiC by Molecular Doping. *Phys. Rev. B* **2010**, *81*, 235401.
8. Lee, B.; Chen, Y.; Duerr, F.; Mastrogiovanni, D.; Garfunkel, E.; Andrei, E. Y.; Podzorov, V. Modification of Electronic Properties of Graphene with Self-Assembled Monolayers. *Nano Lett.* **2010**, *10*, 2427–2432.
9. Whitesides, G. M.; Mathis, J. P.; Seto, C. T. Molecular Self-Assembly and Nanochemistry - A Chemical Strategy for the Synthesis of Nanostructures. *Science* **1991**, *254*, 1312–1319.
10. Ulman, A. *An Introduction to Ultrathin Films*; Academic Press: San Diego, CA, 1991.
11. Woodward, J. T.; Ulman, A.; Schwartz, D. K. Self-Assembled Monolayer Growth of Octadecylphosphonic Acid on Mica. *Langmuir* **1996**, *12*, 3626–3629.
12. Neves, B. R. A.; Salmon, M. E.; Russell, P. E.; Troughton, E. B. Spread Coating of OPA on Mica: From Multilayers to Self-Assembled Monolayers. *Langmuir* **2001**, *17*, 8193–8198.
13. Fontes, G. N.; Malachias, A.; Magalhaes-Paniago, R.; Neves, B. R. A. Structural Investigations of Octadecylphosphonic Acid Multilayers. *Langmuir* **2003**, *19*, 3345–3349.
14. Fontes, G. N.; Neves, B. R. A. Effects of Substrate Polarity and Chain Length on Conformational and Thermal Properties of Phosphonic Acid Self-Assembled Bilayers. *Langmuir* **2005**, *21*, 11113–11118.
15. Cleveland, P.; Anczykowski, B.; Schmid, A. E.; Elings, V. B. Energy Dissipation in Tapping-Mode Atomic Force Microscopy. *Appl. Phys. Lett.* **1998**, *72*, 2613–2615.
16. Groszek, A. J. J. Selective Adsorption at Graphite/Hydrocarbon Interfaces. *Proc. R. Soc. London* **1970**, *314*, 473–498.
17. Casiraghi, C.; Pisana, S.; Novoselov, K. S.; Geim, A. K.; Ferrari, A. C. Raman Fingerprint of Charged Impurities in Graphene. *Appl. Phys. Lett.* **2007**, *91*, 233108.
18. Tuinstra, F.; Koenig, J. L. Raman Spectrum of Graphite. *J. Chem. Phys.* **1969**, *53*, 1126–1130.
19. Cancado, L. G.; Reina, A.; Kong, J.; Dresselhaus, M. S. Geometrical Approach for the Study of G′ Band in the Raman Spectrum of Monolayer Graphene, Bilayer Graphene, and Bulk Graphite. *Phys. Rev. B* **2008**, *77*, 245408.
20. Das, A.; Pisana, S.; Chakraborty, B.; Piscanec, S.; Saha, S. K.; Waghmare, U. V.; Novoselov, K. S.; Krishnamurthy, H. R.; Geim, A. K.; Ferrari, A. C.; et al. Monitoring Dopants by Raman Scattering in an Electrochemically Top-Gated Graphene Transistor. *Nat. Nanotechnol.* **2008**, *3*, 210–215.
21. Basko, M. M.; Piscanec, S.; Ferrari, A. C. Electro-Electron Interactions and Doping Dependence of the Two-Phonon Raman Intensity in Graphene. *Phys. Rev. B* **2009**, *80*, 165413.
22. Brey, L.; Fertig, H. A. Emerging Zero Modes for Graphene in a Periodic Potential. *Phys. Rev. Lett.* **2009**, *103*, 046800.
23. Kohn, W.; Sham, L. J. Self-Consistent Equations Including Exchange and Correlation Effects. *Phys. Rev.* **1965**, *140*, A1133–A1138.
24. Soler, J. M.; Artacho, E.; Gale, J. D.; García, A.; Junquera, J.; Ordejón, P.; Sánchez-Portal, D. The SIESTA Method for *Ab Initio* Order-N Materials Simulation. *Condens. Matter* **2002**, *14*, 2745–2779.
25. Kleinman, L.; Bylander, D. M. Efficacious Form for Model Pseudopotentials. *Phys. Rev. Lett.* **1982**, *48*, 1425–1428.